Atmos. Chem. Phys. Discuss., 10, 30731–30776, 2010
www.atmos-chem-phys-discuss.net/10/30731/2010/
doi:10.5194/acpd-10-30731-2010

Atmospheric Chemistry and Physics Discussions

Global and regional trends in aerosol optical depth based on remote sensing products and pollutant emission estimates between 2000 and 2009

A. de Meij[1], **A. Pozzer**[1], **and J. Lelieveld**[1,2]

[1]Energy, Environment and Water Research Centre, The Cyprus Institute, 20 Kavafi Street, 1645, Nicosia, Cyprus
[2]Max Planck Institute for Chemistry, Becherweg 27, 55128 Mainz, Germany

Received: 11 October 2010 – Accepted: 6 December 2010 – Published: 17 December 2010

Correspondence to: A. de Meij (a.demeij@cyi.ac.cy)

Published by Copernicus Publications on behalf of the European Geosciences Union.

Abstract

This study evaluates global and regional aerosol optical depth (AOD) trends in view of aerosol (precursor) emission changes between 2000 and 2009. We use AOD products from MODIS, MISR and AERONET, and emission estimates from the EMEP, REAS and IPCC inventories. First we compare trends in global Level 3 AOD products of MODIS, MISR and AERONET (Level 2). We find generally negative trends over Europe and North America, whereas over South and East Asia they are mostly positive. The negative trends over parts of Europe and North-East America appear to be significant. Second, we analyze MODIS Level 2 AODs for three selected regions with good data coverage (Central Mediterranean, North-East America and East Asia) and compare with Level 3 products. This corroborates that the 2000–2009 AOD trend over the Central Mediterranean is negative and corresponds well with the MODIS Level 3 analysis. Also for North-East America the trend is generally negative and in agreement with MODIS Level 3 products. For East Asia the trends derived from Level 2 products are mostly positive and correspond with the MODIS Level 3 results. Over Europe, the trends in aerosol single scattering albedo, as derived from MISR data, appear to be positive (declining solar radiation absorption), whereas this is not the case over the USA, though these data are not yet validated. Third we compare trends in AOD with emission changes of SO_2, NO_x, NH_3 and black carbon. We associate the downward trends in AOD over Europe and North America with decreasing emissions of SO_2, NO_x, and other criteria pollutants, and consequently declining aerosol concentrations. Over East Asia the MODIS Level 2 trends are generally positive, consistent with increasing pollutant emissions by fossil energy use and growing industrial and urban activities. It appears that SO_2 emission changes dominate the AOD trends, although especially in Asia NO_x emissions may become increasingly important. Our results suggest that solar brightening due to decreasing SO_2 emissions and resulting downward AOD trends over Europe may have weakened in the 2000s compared to the 1990s.

ACPD

10, 30731–30776, 2010

1 Introduction

The concentration changes of atmospheric aerosols cause radiative forcings of climate, known as the aerosol direct effect, and may modify cloud properties, known as aerosol indirect effects (Ramanathan et al., 2001a,b; Kaufman et al., 2002). Depending on their composition, aerosols scatter (e.g. sulfate) and absorb (e.g. black carbon) sunlight, mostly cooling the Earth's surface. Recent studies focusing on the Northern Hemisphere (Wild et al., 2005; Wild, 2010, and references therein) have shown that since the late 1980s the decline in solar radiation at the Earth's surface due to aerosol pollution (dimming) has reversed. This change from dimming to brightening has important consequences for climate change, affecting the hydrological cycle, cloud formation processes and surface temperatures, possibly intensifying the warming trend caused by CO_2 and other greenhouse gases.

Several studies have investigated the global and regional surface solar radiation budget using data of the Global Energy Balance Archive (GEBA), such as Ohmura (2009), Gilgen et al. (2009), Long et al. (2009), Norris and Wild (2009). Pinker et al. (2005) and Hinkelman et al. (2009) analyzed long-term variations in solar radiation at the Earth's surface using satellite data. Mishchenko et al. (2007) use Aerosol Optical Depth (AOD) from the Advanced Very High Resolution Radiometer (AVHRR) satellite to study the dimming and brightening tendencies. The AOD is the integral of the extinction (scattering plus absorption) by the aerosols over the atmospheric column, and trends have been shown to be largely anthropogenic (Streets et al., 2009). Remer et al. (2008) analyzed Moderate resolution Imaging Spectroradiometer (MODIS) Terra and Aqua Level 2 and Level 3 aerosol products over land and the ocean for 2002–2006. They found elevated AODs over India and East Asia and reduced AODs over North America and Europe. Chylek et al. (2007) analyzed Multi-angle Imaging Spectro Radiometer (MISR) AODs for 2000–2006 and found a decrease over the USA of −0.0073/yr and over the Northern Hemisphere of −0.0014/yr. Lu et al. (2010) studied the SO_2 emission trend in China after 2000 and found a positive relation with observed Level 3 AODs of

ACPD
10, 30731–30776, 2010

the MODIS and MISR instruments. A modeling study by Streets et al. (2006) showed that the trends in surface radiation are correlated with the trends in calculated emissions of sulfur dioxide (SO_2), black carbon (BC) and AODs. Zhang and Reid (2010) analyzed global and regional trends in AOD of MODIS and MISR over the oceans, using Level 2 products. They show that for both instruments a statistically negligible global trend of 0.0003/yr is found, with strong regional trends over the Bay of Bengal (0.07/decade), the east coast of Asia (0.06/decade) and the Arabian Sea (0.06/decade) by MODIS and MISR. Kishcha et al. (2009) studied the meridional distribution of AODs over the ocean between 2000 and 2008 using MODIS and MISR products. They concluded that the brightening phenomenon over land was not observed over the oceans at mid-latitudes (30°–60° N).

To our knowledge no work has been reported comparing the AOD trends of the MODIS and MISR measurements with data of the AERONET network for the period 2000–2009 on global (using Level 3 products) and regional scales (also using Level 2 products), and comparing these trends to aerosol (precursors) emissions.

This study has three main objectives. The first is to compare trends in global Level 3 AOD products of MODIS, MISR and AERONET (Level 2) for the period 2000–2009. Using Level 3 data gives a first impression of the trend. However, it is not recommended to draw strong conclusions based on Level 3 data products, because the sampling of actual retrievals is highly non-uniform in space and time, even at the resolution of these products (MODIS 1°×1° and MISR 0.5°×0.5°) (Kahn et al., 2009). Therefore our second objective is to also analyze MODIS Level 2 AODs between 2000 and 2009 for three selected regions with good data coverage and compare the trends with MODIS Level 3 data. The advantage of Level 2 is that it provides information about the sampling time and has a better spatial representation (10×10 km), which is relevant for the comparison to AERONET observations. The three regions are i) the Mediterranean area (min/max longitude 5.0°; 27.0°; min/max latitude 34.0°; 46.0°), which is indicated in the IPCC (2007) report (4AR) as an area vulnerable to climate change, ii) the eastern part of North America (min/max longitude −85.0°; −70.0°; min/max latitude 30.0°; 47.0°)

ACPD
10, 30731–30776, 2010

and iii) the north eastern part of China (min/max longitude 103.0°;127.0°; min/max latitude 20.0°; 44.0°), i.e. densely populated areas with intense industrial activities.

Our third objective is to compare the trends in AODs with the trends in emissions of SO_2, which contribute substantially to the global AOD (Streets et al., 2006), nitrogen oxides (NO_x), ammonia (NH_3) and black carbon (BC). For this purpose we analyze estimated source strengths for the years 1990, 1995, 2000, 2005 and 2010 from global and regional emission inventories.

2 Methodology

Satellite data of the Multi-angle Imaging Spectro Radiometer (MISR) and MODerate resolution Imaging Spectro radiometer (MODIS) are used for quantitative comparisons with the sun photometer data of the AErosol RObotic NETwork (AERONET). MISR and MODIS are both on NASA's Earth Observing System (EOS) Terra platform, launched in December 1999. First we evaluate the global AOD trends from the MODIS and MISR Level 3 products by analyzing the change in the AODs between 2000 and 2009. Second, we compare the monthly mean Level 3 AODs between MODIS and MISR for 152 locations. We identify within the MODIS and MISR Level 3 data sets the geographical pixel location of the AERONET station and we extract the AODs. In Fig. 1 an overview of the AERONET stations is given (blue and red dots) for which we compare with MODIS and MISR data for the period February 2000–December 2009. Third we select the AERONET stations for which sufficient AERONET daily Level 2 data is available (>50 months) and compare these AOD profiles with MODIS and MISR (62 stations, red dots). Fourth we analyze the AOD trend of MODIS Level 2 product for three regions and compare the results with MODIS Level 3 data. For MODIS Level 2 we extract from the overpasses the AODs within the geographical range of ±15×30 km around the AERONET station.

For this study MISR AOD products are available from February 2000 to November 2009 and MODIS AOD products from February 2000 to December 2009. For MODIS

ACPD
10, 30731–30776, 2010

collection 5.0 Level 2 and Level 3 data is used, for MISR F15 Level 3 and for AERONET Level 2 data. More details regarding the satellites and the AERONET network are given in Sect. 2.1.

Finally we compare the AOD trends with emission estimates of SO_2, NO_x, NH_3 and BC for the years 1990, 1995, 2000, 2005 and 2010 for the different regions. The emission estimations are taken from the Co-operative Programme for Monitoring and Evaluation of the Long-range Transmission of Air Pollutants (EMEP) for Europe, the Region Emission Inventory for Asia (REAS) and the Intergovernmental Panel on Climate Change (IPCC, RCP 3PD) for North America and the entire globe.

2.1 Description of the data sets

2.1.1 AERONET

The sun photometer data used in this study have been obtained by Cimel instruments which are part of the AERONET global network (Holben et al., 1998). AERONET data are widely used as a reference for satellite validation and model evaluation studies, because the measurement characteristics are well understood (Dubovik et al., 2000). The sun photometer measures the attenuation (every 15 min) in a 1.2 degree field of view, at eight solar spectral bands (340, 380, 440, 500, 670, 870, 940 and 1020 nm). The solar extinction measurements are used to calculate for each wavelength the aerosol optical depth with an accuracy of about 0.01–0.02 AOD units (Eck et al., 1999). Sun photometers acquire aerosol data only during daylight and in clear sky conditions. In this work the cloud-screened monthly mean Level 2 data are used. Data is obtained from the website: http://aeronet.gsfc.nasa.gov/.

We use AOD at 550 nm (the solar irradiance is most intense in the green/yellow part of the spectrum around 550 nm) calculated from the AOD values reported at 870 and 440 nm by using the information of the Ångström coefficient (α). This allows us to compare AERONET AOD with MODIS (550 nm) and MISR AOD (555 nm).

ACPD
10, 30731–30776, 2010

The AOD values of the AERONET dataset are interpolated to 550 nm. First the Ångström coefficient is calculated by using two wavelengths (870 nm and 440 nm, see Eq. 1). Then the AOD (τ) at 550 nm is calculated (Eq. 2).

$$\alpha = -\ln[\tau(0.440)/\tau(0.870)]/\ln(0.44/0.87) \quad (1)$$

$$\tau(550) = \exp\{-\alpha^* \ln(0.55/0.44) + \ln[\tau(440)]\} \quad (2)$$

2.1.2 MISR

The Multi-angle Imaging Spectro-Radiometer (MISR) (Diner et al., 1998) has four forward looking cameras, one nadir and four backward looking (at viewing angles of 70.5°, 60.0°, 45.6°, 26.1°, and 0°), and each camera measures in four different wavelengths centered at 446 nm (blue), 558 nm (green), 671 nm (red) and 866 nm (near-infrared). The AOD in the Level 2 data is reported at 17.6×17.6 km resolution, by analyzing top-of-atmosphere radiances from 16×16 pixels patches of 1.1 km resolution (Martonchik et al., 2009; Diner et al., 2009; Kahn et al., 2009). This feature of observing at different angles enables retrieval of total-column AOD, which is defined as the integral of aerosol extinction from the surface to the top of the atmosphere, and aerosol type over both land and ocean (Martonchik et al., 2009). There is a time difference of 7.5 min between the first and the last camera recording to view the exact geographic position as the satellite passes over. Each path has a swath width of 360 km with a 16-day repeat cycle. In this work global Level 3 CGAS-F15 products are used (Optical Depth Average), which are derived from Level 1 and Level 2 products, and are averaged over a month, season or year. Level 3 product files contain AOD at 558 nm and the products are stored on a geographic grid of 0.5×0.5 degrees. A comparison over land and ocean with AERONET data showed that MISR AODs are within 0.05 or 20% of that of AERONET (Kahn et al., 2005, 2010). MISR AODs are obtained from https://wist.echo.nasa.gov/api/.

ACPD
10, 30731–30776, 2010

2.1.3 MODIS

The MODerate resolution Imaging Spectro-radiometer (MODIS) has one camera, measuring radiances in 36 spectral bands, from 0.4 µm–14.5 µm with spatial resolutions of 250 m (bands 1–2), 500 m (bands 3–7) and 1000 m (bands 8–36). Daily Level 2 (MOD04) aerosol optical thickness data (550 nm) are produced on the spatial resolution of 10×10 km over land, using the 1 km×1 km cloud-free pixel size. The MODIS Level 2 product refers to a swath width of about 2330 km, therefore the instrument has almost daily global coverage. MODIS aerosol products are provided over land (Kaufman et al., 1997) and water surfaces (Tanré et al., 1997). In this work both Level 2 and global Level 3 (MOD08) Collection 005 products are used (Optical_Depth_Land_And_Ocean_Mean). The latter is derived from the statistics of the Level 2 products and stored on a 1×1 degree equal-angle grid in the MOD08 Level 3 product file. Reported MODIS aerosol uncertainties over land are $\Delta\tau = \pm 0.05 \pm 0.151^{*}$AOD (Remer et al. 2008; Levy et al., 2010). There is no aerosol retrieval possible over bright surfaces, such as deserts and ice. MODIS AODs can be obtained from https://wist.echo.nasa.gov/api/.

2.1.4 Emission inventories

In this study we use independent emission inventories to estimate the total sources of anthropogenic SO_2, NO_x, NH_3 and BC for 1990, 1995, 2000, 2005 and 2010. Below a brief description of the emission inventories is given.

2.1.4.1 EMEP emission inventory

The Co-operative Programme for Monitoring and Evaluation of the Long-range Transmission of Air Pollutants in Europe (EMEP) evaluates air quality in Europe by operating a measurement network, as well as performing model assessments. The EMEP emission inventory (http://www.ceip.at/) contains reported anthropogenic emission data for

ACPD
10, 30731–30776, 2010

each European country, complemented by expert judgments when incomplete or erroneous data reports are detected. The 50 km×50 km emission inventory contains SO_2, NO_x, NH_3, NMVOC, CO, $PM_{2.5}$ and PM_{10} for 11 CORINAIR source sectors (Vestreng et al., 2007, 2008).

2.1.4.2 REAS emission inventory

For Asia we use the anthropogenic emissions of SO_2 and BC of the Region Emission Inventory for Asia (REAS), Ohara et al. (2007), http://www.jamstec.go.jp/frcgc/research/p3/emission.htm. The REAS inventory includes NO_x, SO_2, CO, BC, OC, CO_2, N_2O, NH_3, CH_4, and NMVOC from anthropogenic activities (combustion, non-combustion, agriculture, and others) on a 0.5°×0.5° resolution. Open biomass burning is not included in REAS.

2.1.4.3 IPCC emission inventory

For North America and global sources of trace species we use the historical and projected Intergovernmental Panel on Climate Change (IPCC) emission estimates, which include both anthropogenic and biogenic emissions. We use the Representative Concentration Pathways (RCPs) 3-PD emission scenario (Vuuren et al., 2007), which is to be used in the IPCC 5th Assessment Report (AR5). This scenario is developed by the IMAGE modeling team of the Netherlands Environmental Assessment Agency. The number of the RCP scenario represents the radiative forcing level in 2100.

The IPCC emission inventory includes international shipping emissions; ship emission totals for the year 2000 are taken from Table 3 of Eyring et al. (2010). Historical CO_2 ship emission totals from 1850 to 2000 are based on the Second International Maritime Organization (IMO) GHG Study (Buhaug et al., 2009). Historical non-CO_2 shipping emission totals are scaled backwards in time by using the IMO CO_2 emission time series. Aviation emissions are based on Lee et al. (2009). Sulfur emissions of all other sectors, both historical and year 2000 emissions, are from Smith et al. (2010).

ACPD
10, 30731–30776, 2010

Black and organic carbon emissions of all other sectors, both historical and year 2000 emissions are from Bond et al. (2007). NO_x and NH_3 emissions of all other sectors are from Lamarque et al. (2010). The emissions estimates are provided on a 0.5°×0.5° latitude/longitude resolution.

3 Results

In Sect. 3.1 we analyze global AOD trends by MODIS and MISR and we determine their significance. In Sect. 3.2 we analyze MODIS Level 3 and MISR Level 3 monthly mean AODs between 2000 and 2009 for 152 locations. In Sect. 3.3 we include the AERONET daily Level 2 products, followed by analyzing MODIS Level 2 data for three selected regions between 2000 and 2009 in Sect. 3.4. In the same section we explain the increase or decrease in the AOD trends by analyzing the emission trends of SO_2, NO_x, NH_3 and BC for these three regions.

3.1 Global AOD trends by MODIS and MISR and their significance

In Fig. 2 the slopes of the linear trend per year of the global AOD between 2000 and 2009 for MODIS (a) and MISR (b) are presented, together with the difference based on the slope of the AOD between 2000 and 2009 for the two instruments (c and d). The negative trends in the MODIS and MISR AODs between 2000 and 2009 are indicated in blue and the positive trends in red. Areas presented in white indicate that the annual AOD trend is insignificant, i.e. between −0.001 and 0.001 (Fig. 2a,b,e,f), the change in the AOD is between −0.02 and 0.02 (Fig. 2c,d), or no data is available (due to the limitations of the MODIS instrument over bright surfaces, such as deserts and snow covered areas) or less than 80 data points (months) per grid cell are available. For Europe and North-East America the changes in AOD are negative (up to −0.12 AOD in Europe by MODIS), indicating a significant decrease of the AOD in about a decade. The decrease over North America by MODIS agrees with the analysis of Chylek et al. (2007), about

ACPD
10, 30731–30776, 2010

−0.007/yr. MISR registers a decrease over parts of Europe and the eastern part of North America, however more to the west (e.g. parts over the Rocky Mountains and Canada) a positive trend is observed. The differences in AOD trends between MODIS and MISR could be related to i) the difference in cloud screening, ii) the number of days for obtaining global coverage (difference in swath width between the instruments results in fewer data points by MISR to construct a monthly average). Analyzing the number of months for which AOD data is available, we see that MODIS has more valid months for which AODs are available than MISR over the eastern part of North America, Europe, Amazon Forest, Central Africa, Indonesia and South East Asia (not shown). iii) Difference in sampling coincidence, iv) the fact that MISR provides radiance measurements at nine different viewing angles compared to one (nadir) on MODIS. This gives MISR greater sensitivity to thin aerosol layers, especially over bright land surfaces. Finally v) other algorithmic issues occur for MODIS and MISR (e.g., Levy et al., 2010; Kahn et al., 2010) that can also contribute to differences. For example, the current MISR algorithm does not account for mixtures of biomass burning and dust aerosols and tends to overestimate AOD in such situations, whereas MODIS tends to overestimate AOD over bright surfaces (Kahn et al., 2009).

Over India and parts of China the changes in AOD are positive by MODIS and MISR, up to 0.2 (~0.01/yr) in the northeastern part of China. Interesting is the increase in AODs by the two instruments over the Bay of Bengal and the Arabian Sea region (up to 0.009/yr), which is in line with the study of Zhang and Reid (2010). They found increasing trends from MODIS data over the Bay of Bengal, Arabian Sea of 0.07 and 0.06 per decade, respectively. These increases can be explained by the transport of air pollution from the adjacent continents (Leon et al., 2001; Heymsfield and McFarquhar, 2001; Ramanathan et al., 2001a; Lelieveld et al., 2001).

We have seen above that satellite observed AODs during the 2000–2009 period indicate a positive AOD trend over Eastern Asia and a negative trend over Europe and North-East USA. These trends can be related to aerosol (precursors) emissions, which will be discussed in Sect. 3.4.

ACPD
10, 30731–30776, 2010

Here we determine the significance of these trends by analyzing global MODIS and MISR Level 3 products.

A trend is significant at a confidence level of 95% when $|\frac{\omega}{\sigma_\omega}|$, where ω is the yearly trend estimate and σ_ω is the standard deviation of the trend estimate. σ_ω and ω have been estimated using the method of Weatherhead et al. (1998) and references therein.

In Fig. 2e,f we present the significance of the MODIS and MISR Level 3 AOD trend between 2001 and 2009 (only slopes >0.001) with confidence level >95%. We selected 2001 to have a full year of data, which is not the case for 2000. Over the Eastern USA and Europe the negative trend in the AODs is significant (blue), which appears to be related to the reduction of SO_2 and NO_x emissions, see Sect. 3.4. Significant positive trends are found over the Bay of Bengal, Arabian Sea and the Arabian Gulf region (red, yellow) which are related to the transport of anthropogenic air pollution origination from the adjacent continental regions, as mentioned earlier. Over large parts of Asia (i.e. Northern India and Eastern China) no significant positive trends are found, which corroborates the AERONET trends based on Daily Level 2 data, and will be further discussed in Sect. 3.3. South of Hawaii both MODIS and MISR show a significant positive trend. Analyzing the temporal profile of the AOD around Hawaii, we see a strong increase in the AOD in March and April 2008. The reason for the increase is the eruption of the Kilauea volcano in Hawaii on March 19 2008. The eruption of the volcano led to a strong increase in SO_2 and volcanic ash emissions and consequently increasing AODs, which has been observed by satellites (http://earthobservatory.nasa.gov/NaturalHazards/view.php?id=19711&oldid=14759).

Over other regions such as the west coast of Southern Africa, Russia, Central America, Central Africa, parts over the Atlantic Ocean and the northeastern part of Australia, significant AOD trends with a high confidence level (positive or negative) are observed, primarily in the better-sampled MODIS data.

ACPD
10, 30731–30776, 2010

3.2 Regional AOD trends by MODIS and MISR

In this section we compare the AOD trends between MODIS and MISR Level 3 for the 152 locations, as presented in Fig. 1. The locations correspond with the locations of AERONET stations from which data will be used to compare the MODIS and MISR AOD trends in Sect. 3.2.

3.2.1 Europe

In Fig. 3 the slope of the linear AOD trend for each station is given. The diameter of the circle indicates the magnitude of the slope, see Table S1 of the electronic supplement. Blue and green circles represent negative trends by MODIS and MISR, respectively. Orange and red represent positive trends by MODIS and MISR, respectively. The slope of the trend line is calculated from the linear regression of the AOD trend and the absolute difference of the AOD is the difference between the maximum and minimum value of the regression line.

In general both MODIS and MISR show an overall negative AOD trend between 2000 and 2009 over Europe (46 locations) of −32% (−0.06 AOD, slope -4.72×10^{-4}) and −7% (−0.01 AOD, slope -1.30×10^{-4}), respectively (Fig. 3a and Table 1). Comparing the AOD trend between MODIS and MISR we find that for ∼83% of the locations the trends are similar (negative). MODIS shows a negative AOD trend for almost all the locations in Europe (except Mace Head, Ireland), whereas MISR shows a positive trend for 14 stations (Table S1). In general MODIS shows a larger negative trend than MISR. An explanation for the observed AOD reductions could be a decrease of the anthropogenic emissions of SO_2, NO_x, NH_3 and BC and related pollutants, associated with the implementation of air pollution legislation (Sect. 3.3).

For the SMHI station in Norrkoping (SE) on May 2005 MISR produces an outlier in the AOD of 0.61, which is a factor 7 higher than the 10-year average, leading to an unexpected large overall positive trend of 8%. When this outlier is excluded the positive trend reduces to ∼3%. This suggests that the sampling frequency might be

ACPD
10, 30731–30776, 2010

too low for this station. For the stations in Eastern Europe, both MODIS and MISR show a negative trend, but for one location (Kiev) MISR indicates a positive trend of 17% (0.025 AOD). The differences in AOD trends between MODIS and MISR could be related to the difference in cloud screening and the number of days for obtaining global coverage, as mentioned earlier.

We clearly see a seasonal cycle with elevated AODs in the summer period (not shown). The reasons could be (i) the enhanced formation of secondary aerosols during summer, i.e. photochemical oxidation of SO_2 to sulfate and NO_x to nitrate, (ii) aerosols from biomass burning (dry season), (iii) long-distance dust intrusions from the Saharan desert, and (iv) less efficient removal of aerosols by precipitation compared to the winter. The contribution of Saharan dust to the total AOD is profound for the stations around the Mediterranean area during spring and summer (Dayan et al., 2008; De Meij and Lelieveld, 2010). In general MODIS AOD is higher than of MISR over land, which has been previously noted in other studies e.g., Abdou et al. (2005). Minimum monthly mean AODs are between 0.07 and 0.11.

Analyzing the MISR Level 3 single scattering albedo (SSA) for Forth Crete, Rome Tor Vergata, Lecce University, OHP observatoire, Birkenes, Xanthi, Bucarest and Tuz Gulu (for these stations substantial SSA data is available), we observe a generally positive trend in the SSA between 2000 and 2009. This indicates a decrease in sunlight absorbing material (BC, dust). This could be explained by the increased implementation of soot filters on diesel engine vehicles and the improvement of combustion technology. Only for Valladolid, Kiev and Moldova the trends in SSA are negative, indicating an increase in absorbing aerosols over these areas. Although these trends follow the expectation based on emission estimates, it is not recommended to draw strong conclusions using MISR SSA products, because a limited selection of absorbing particles are included in the current algorithm, aerosol mixtures of BC and dust are not included, and the MISR SSA values are not validated (Kahn et al., 2010).

ACPD
10, 30731–30776, 2010

3.2.2 North America

For North America both MODIS and MISR show a decrease in the AOD, of −25% (−0.043 AOD, slope -3.42×10^{-4}) and −13% (−0.017 AOD, slope -1.46×10^{-4}), respectively (Table 1). For almost all locations (40) MODIS indicates a negative trend of which 27 are corroborated by the MISR measurements (Fig. 3b and Table S1). Only for one location (Rimrock) MODIS shows a positive trend (7%, 0.006 AOD, slope 5.16×10^{-5}). For 13 locations MISR shows a positive trend, of which some are significant. Both instruments indicate a negative trend over the eastern part of North America. Again the deviations in slope (negative or positive) between MODIS and MISR could be related to differences in locations and sampling coincidences of the data used to construct the monthly averages, and the cloud screening algorithms.

Also for North America we observe a seasonal cycle in the AOD (not shown), with peak values during summertime, similar to the cycle over Europe. Minimum AODs are between 0.05 and 0.10, which is somewhat lower than the minimum AODs found for Europe. Again, MODIS AOD is higher than of MISR. The negative trends by MODIS and MISR are somewhat smaller than those over Europe.

For North America we have a sufficient MISR Monthly Level 3 data volume of SSA available for Biggs, Table Mountain, Oklahoma State University, Kellog LTER, Columbia Science Centre, Burtonsville, Calipso Wilston LK, Jones RC, Sioux Falls, and Los Alamos. Only for Biggs and Los Alamos the trends in SSA between 2000 and 2009 are positive. This means that for all other locations relatively more light absorbing aerosols are found. This deviates from the overall trend in Europe.

3.2.3 South America

MODIS generally shows a negative trend of −11% (−0.020 AOD, slope -2.05×10^{-4}) for the 15 locations considered, whereas MISR shows a small upward trend of 5% (0.008 AOD, slope 6.40×10^{-5}). Analyzing the AODs of MODIS in Fig. 3c and Table S1 indicates that for five locations in Brazil the trends are positive, i.e. Abracos Hill, Alta

ACPD
10, 30731–30776, 2010

Foresta, Uberlandia Rio Branco and Tukuri. For Tukuri in December 2009 an outlier of 1.65 AOD occurs (not shown). By excluding this outlier the AOD trend becomes negative. MISR shows a positive trend for ten locations, while for seven of them MODIS shows a negative trend. Both MODIS and MISR indicate high AODs (up to 1.6) between August and October for Alta Foresta, Cuiaba-Miranda, Abracos Hill and Rio Branco (not shown). Between August and October biomass burning (deforestation fires as well as sugar cane agricultural burning) lead to high AODs with peak values up to 1.0. Minimum AODs are observed during the wet season (November–May) when the aerosols are washed out from the atmosphere and burning is at minimum.

3.2.4 Africa

In general the AOD trends for the 8 locations in Africa by both MODIS (−18%; −0.063 AOD, slope -5.0×10^{-4}) and MISR (−6%; −0.023 AOD, slope -3.0×10^{-4}) are negative, however for some stations the slope of the trend line is positive. Biomass burning is common practice in many regions in Africa, which is represented in the yearly cycles of high AODs ranging between 0.5 and 1.0 (not shown). High AODs are observed by both satellite instruments for Djougou (Benin) in February-March, Lamto (Ivory Coast) in January–March, Ilorin (Nigeria) in January–March, Burkina Fasso in April–June, and Kasama (Zambia) in September-October.

3.2.5 Asia

The AOD trends in Asia derived from MODIS data are generally negative (−2%; −0.007 AOD, slope -5.04×10^{-5}) and for MISR positive (11%; 0.032 AOD, slope 2.69×10^{-4}). Analyzing the trend for the 32 locations in Asia (Fig. 3e and Table 1), we see that MODIS shows a positive trend for 12 locations and MISR for 23 locations. The two instruments show the same sign for 18 locations (negative or positive). In Fig. 3e we see a strong positive trend for both instruments over the east coast of China and the northern and eastern part of India, indicated by the orange (MODIS) and red

ACPD
10, 30731–30776, 2010

circles (MISR). The likely reason is the growth of SO_2 and other pollutant emissions by industrial activities (Cofala et al., 2004; Streets and Waldhoff 2000; Garg et al., 2000; Lei et al., 2010). More details are given in Sect. 3.4. For 11 stations in China we derive a generally upward AOD trend by MISR, and only for two stations the trends are negative Jingtai (−7%, −0.021 AOD) and Liangning (−4%, −0.008 AOD). MODIS shows a negative trend for four locations, i.e. Asia1 (−18%, 0.006 AOD), Jingtai (−6%, −0.021), Lhasa (−30%, −0.046) and Hefei (−3%, −0.025). For Dunhuang (CN) there is no data available for MODIS, because it is located in the desert of the Gansu province in China and the MODIS algorithm has difficulties in retrieving aerosol optical properties over bright surfaces. For the stations in China MISR Monthly Level 3 SSA trends are negative, indicating an increase in absorbing aerosols. The differences in AOD between MODIS and MISR could be related to e.g. the difference in cloud screening and sampling, as mentioned earlier.

The AOD trends in India are positive in four locations for both MODIS and MISR, and only for Chitkara (North-West India) the trend is negative. For Kanpur, Vishkhapatnam, Chitkara and Gandhi College the AODs are high (decadal average >0.4), with peak values up to 1.53 by MODIS for Chitkara. In India power plants and associated fossil fuel consumption by industry and additionally by transport are responsible for a strong increase in SO_2 and other pollutant emissions (Garg et al., 2000). Uttar Pradesh, located in the north of India is the most highly populated state of the country with about 190 million people. Emissions appear to be closely linked to the population growth (IPCC, 2007, WG1-AR4). Both MODIS and MISR indicate a positive trend for the stations Kanpur and Gandhi College, which are located in Uttar Pradesh province. Analyzing the MISR Monthly Level 3 SSA for Dharwar, Viskhapatnam, Chitkara, Kanpur, Gandhi College indicates that only for Dharwar the SSA trend is negative. This indicates that in general the upward trend of absorbing aerosols (black carbon) is less (or even downward) compared to scattering aerosols in India, which could be related to the stricter implementation of air pollution legislation for commercial diesel engine vehicles since 2000 in order to improve air quality. High SSA's are found (>0.98) for

ACPD
10, 30731–30776, 2010

Kanpur and the other stations, which corresponds with Dey and Di Girolamo (2010). They found that MISR overestimate SSA for India, because the current algorithm does not account for aerosol mixtures of BC and dust.

For the Siberian sites (Tomsk, Irkutsk and Yaktusk) MODIS registers negative trends (-1.47×10^{-4}, -9.85×10^{-4} and -1.04×10^{-4}, respectively), while MISR shows a positive trends (4.80×10^{-5}, 4.38×10^{-4} and 2.03×10^{-4}, respectively). Both instruments are "blind" during winter, due to snow/ice (bright) surfaces and cloud cover. In Osaka (Japan) both instruments indicate a significant reduction in AOD, which is related to the reduction in emissions since the 1990s (Cofala et al., 2004; Nurrohim and Hiroshi, 2003). This reduction in AOD confirms the finding by Lu et al. (2010), who emphasized the nationwide SO_2 reduction in Japan, in response to the national air pollution legislation. However, long-range transport of SO_2 from China can contribute to air pollution in Japan, possibly contributing to a slowdown of the negative trend (Lu et al., 2010).

The generally more negative trends shown by MODIS as compared to MISR at nearly all sites could be related to sampling differences between the two instruments (Zhang and Reid, 2010).

On average MODIS AOD is a factor 1.4 higher than MISR AOD for Asia. The minimum AODs by MODIS range between 0.3 and 0.38, which is a factor 1.5 higher than the minimum AODs by MISR (0.2–0.3). MODIS collection 5 tends to overestimate AOD over bright surfaces (Levy et al., 2010). A low bias in MISR AOD appears for AOD >~0.4, and increases with increasing AOD (Kahn et al., 2005, 2010; Di Girolamo et al., 2004). Both the MODIS and MISR artifacts contribute to the systematic difference in trend magnitudes.

3.2.6 Australia

For Australia we examine 8 locations. On average MODIS indicates a negative trend of −43% and MISR a positive trend of 2%. MODIS indicates a negative trend for the 8 locations, whereas MISR shows a negative trend for four locations, i.e. Canberra (−5%, −0.002 AOD), Merredin (−5%, −0.004 AOD), Lake Argyle (−35%, −0.053 AOD)

ACPD
10, 30731–30776, 2010

and Jabiru (−2%, −0.002 AOD). For Canberra we observe in the MISR AOD an outlier of 0.563 on January 2005, while the 2000–2009 average is 0.052. Excluding the outlier changes the trend for Canberra from −5% to +20%. No MODIS data is available for Ting Tingana and Birdsville, because these locations are situated in the Strzelecki Desert and Simpson Desert, respectively and the MODIS algorithm does not retrieve data over bright surfaces.

3.2.7 Middle East

s3.2.7

The number of locations in the Middle East is limited related to the difficulties of MODIS to observe aerosol optical properties over bright surfaces. For 2 stations in the Middle East (Dhabi and Dhadnah) MODIS and MISR show significant positive trends in the AOD. For Nes Ziona (Israel) the trends by both instruments are negative, i.e. −22% (−0.072 AOD, slope -5.67×10^{-4}) for MODIS and −15% (−0.037 AOD, slope -2.76×10^{-4}) for MISR.

3.3 Global AOD trends by MODIS, MISR and AERONET

In this section we analyze the MODIS and MISR AOD trends between 2000 and 2009, together with the AERONET AODs. We selected the 62 locations for which the AERONET stations have at least 50 monthly mean data points. We compare MODIS and MISR AODs with AERONET, starting from the first month for which the AERONET station registers AOD. Therefore the number of months for which AOD data is available for each station can differ. The locations are represented by red dots in Fig. 1.

3.3.1 Europe

In Fig. 4a the AOD trend for 17 locations in Europe is shown as derived from MODIS, MISR and AERONET data. The decrease in AOD between 2000 and 2009 by MODIS (−30%; −0.060 AOD) corresponds well with that by AERONET (−25%; −0.054 AOD),

ACPD
10, 30731–30776, 2010

while the decrease by MISR is smaller (−9%; −0.014 AOD), see Table 1b. MODIS, MISR and AERONET show a negative AOD trend for all locations in Europe (Table S2), except for IMS-METU-ERDEMLI (Turkey). The seasonal cycles in the AOD are clearly discernable and can be related to photochemical oxidation processes, aerosol scavenging by rain, biomass burning and dust transport, as mentioned earlier. Table S3 presents the MODIS, MISR and AERONET average AODs between 2000 and 2009, together with the standard deviations and the temporal correlation coefficients with AERONET and the number of months for which AOD data is available for each station. The decadal overall average of MODIS (0.185±0.074) is a factor 1.2 higher than of MISR (0.153±0.077) and 5% higher than of AERONET 0.176±0.062. The temporal correlation coefficients with AERONET data are 0.72 and 0.54 for MODIS and MISR, respectively. For Eastern Europe the MODIS AOD (0.194±0.108) is again higher than of MISR (0.171±0.084), but corresponds very well with the average by AERONET (0.197±0.086).

In Table S4 we list the linear AOD trends for the AERONET stations, based on the Daily Level 2 product and we compare these to the trends obtained with the Monthly Level 2 products. For 15 stations we derive a similar (negative) trend in the AOD. Only for Barcelona and Mainz the trends are positive for Daily Level 2. Note that the positive trends for these two stations are small (2%). For the East European stations the trends are similar and both AERONET Daily and Monthly Level 2 show a positive trend for the IMS-METU-ERDEMLI station in Turkey.

3.3.2 North America

For North America (Fig. 4b) the general negative trend of −24% (−0.033) by AERONET corresponds well with the negative trend by MODIS (−23%, −0.039). The negative trend by MISR is −10% (−0.014). In the previous section we have seen that MODIS shows a negative trend for almost all locations in North America (39 out of 40). When we analyze the trend for the period for which AERONET registers AOD the trends for two stations change to positive, i.e. Railroad Valley (9%; AOD 0.027) and Missoula

ACPD
10, 30731–30776, 2010

(10%; AOD 0.013). In general the decadal average by MODIS (0.150±0.077) is higher than MISR (0.125±0.075) and is a factor 1.25 higher than AERONET (0.120±0.065), and again the seasonal cycles are clearly discernable. The temporal correlation coefficients with AERONET data are 0.66 and 0.62 for MODIS and MISR, respectively. Comparing the trend between Daily and Monthly AERONET Level 2 we see that for all North American stations a similar trend in the AOD is found (positive or negative), except for Rimrock.

3.3.3 South America

Analyzing the trend for 7 locations in South America we find a negative trend for MODIS (-1.82×10^{-4}, −0.019 AOD), MISR (-9.91×10^{-6}, −0.001 AOD) and AERONET (-2.50×10^{-4}, −0.03 AOD). We derive a strong seasonal cycle in the AOD, related to emissions by biomass burning. For the 7 stations in South America the trends for AERONET Daily (Table S4) and Monthly Level 2 (Table S2) are similar, i.e. either negative or positive. The temporal correlation coefficients with AERONET data are 0.75 for MISR and 0.82 for MODIS.

3.3.4 Africa

MODIS and MISR indicate an average negative trend of −0.11 (−23%) and −0.033 (−7%), respectively. These negative trends are not statistically robust, because of the limited number of stations for which we compare AODs (4). We see a strong seasonal cycle in the AODs, related biomass burning activities and dust events. For Blida the trend is positive using AERONET Monthly Level 2 (Table S2), while for AERONET Daily Level 2 the trend is negative (Table S4). The reason is that in the Daily Level 3 AODs peak values of 1.2 are observed (caused by Saharan dust). These high values are not present in the Monthly mean Level 2 AODs (max is 0.46) and therefore their influence on the trend is less profound.

ACPD
10, 30731–30776, 2010

3.3.5 Asia

The average trends for Asia over 2000–2009 derived from MODIS (−1%, −0.006 AOD), MISR (24%, 0.07 AOD) and AERONET (24%, 0.07 AOD) are generally positive. The difference in the trend for MODIS compared to the previous section is that the time span for which the AODs are analyzed is not the same, and we use fewer stations (7) for our comparison. Here we compare the trends for the months for which we have AERONET data available. MODIS AODs are in general higher than MISR and AERONET AODs. For Kanpur, Beijing, Xianghe, Osaka, Anmyon the trends are similar for AERONET Daily and Monthly products, i.e. both either negative or positive. Only for Dalazanagad (MN) we see a small difference between the two data sets. The trend based on the Monthly Mean product is less than −1% for this station.

For Australia we have only data available for Lake Argyle and Jabiru, which is insufficient for a meaningful comparison.

Overall the AOD trends derived from MODIS, MISR Level 3and AERONET Level 2 data are similar (either negative or positive). As mentioned in the introduction the use of monthly mean Level 3 data does not provide information about the sampling of the satellite products and the grid resolution is too coarse to accurately represent the location of the AERONET station. Therefore we analyze in the next section MODIS Level 2 data for three regions. MODIS Level 2 provides an AOD product on 10×10 km and has (almost) daily global coverage and the sampling times are known. The selected regions are the Central Mediterranean, North-East USA and North-East China.

In summary, there is qualitative agreement among MODIS, AERONET, and MISR for the trends over the 10-year period in most regions examined. Negative trends appear for most of Europe and North-East America, whereas positive trends are generally found over India and parts of China. Note that MISR sampling is insufficient to draw quantitative statistical conclusions about the 10-year trends at most locations (Fig. 2f).

ACPD
10, 30731–30776, 2010

3.4 MODIS Level 2 AOD trend and pollution emissions

In this section we analyze the AOD trends from MODIS Level 2 product data for three regions, i.e. the Central Mediterranean (min/max longitude 5.0°; 27.0°; min/max latitude 34.0°; 46.0°), North-East America (min/max longitude −85.0°; −70.0°; min/max latitude 30.0°; 47.0°) and the eastern part of China (min/max longitude 103.0°; 127.0°; min/max latitude 20.0°; 44.0°), which results in >10 000 data files per region. We analyze the AODs for the locations corresponding to AERONET stations, see Table 2. The numbers of valid observations are included in the table, which depend on the satellite overpass pattern and cloud free days.

3.4.1 Central Mediterranean

In Fig. 5a the change in MODIS Level 2 AOD between 2000 and 2009 is presented for 7 locations. Larger diameter circles represent stronger AOD trends. In Table 2 the actual change and the relative change of the regression line are given for the stations, together with the change in AOD for the Level 3 products. Comparing these changes in the AOD between Level 2 and Level 3, we note that for both product levels the changes are negative and numbers are of the same magnitude. The number of successful AOD retrievals within the selected domain is lower closer to the boundary of the selected domain than at its center. Analyzing in Table S4 the trend of AERONET Daily Level 2 data for those stations for which substantial Daily Level 2 data is available within the domain of interest (Forth Crete, Rome Tor Vergata, Ispra, Venice and Lecce University) we see that the trends are negative, which corroborates at least qualitatively the results from MODIS Level 2 data.

The decrease of the AOD (presumably mainly anthropogenic aerosols) coincides with the implementation of European air quality legislation to reduce the emissions of SO_2 and other so-called criteria pollutants. Since 1990, the emissions of aerosol precursors have dropped, leading to an improvement in air quality and a reduction in AOD. To investigate in more detail the impact of the change in emissions on AODs, we

ACPD
10, 30731–30776, 2010

present in Table 3 the emissions of SO_2, NO_x, NH_3 and anthropogenic black carbon (BC) for Europe, Asia, the USA and globally, for the years 1990, 1995, 2000, 2005 and 2010.

SO_2 and BC are mainly emitted from fossil fuel (coal and petroleum) combustion. NO_x is mainly emitted from road transport and fossil fuel combustion for energy production and NH_3 is mainly emitted from agricultural activities (waste burning and fertilizers) and to a small extent due to the combustion of biofuels for energy use. The amount of NH_3 emitted by agricultural activities is related to the type of fertilizer, meteorological conditions (wet/dry) and soil properties.

Sulfate is produced by chemical reactions in the atmosphere from gaseous precursors. The main sulfate precursor is anthropogenic SO_2. The oxidation of SO_2 in cloud liquid water by H_2O_2 is very fast and is an important source (more than half) of the atmospheric sulfate aerosol (Pandis and Seinfeld, 1989, Seinfeld and Pandis 1998; and references herein), see the reactions below:

$$SO_2 + H_2O \rightarrow HSO_3^- + H^+ \quad \text{(R1)}$$

$$HSO_3^- + H_2O_2 \leftrightarrow SO_2OOH^- + H_2O \quad \text{(R2)}$$

$$SO_2OOH^- + H^+ \rightarrow H_2SO_4 \quad \text{(R3)}$$

The sulfate produced in reaction 3 can react with ammonia to form ammonium sulfate aerosol according to the reaction:

$$H_2SO_4 + 2NH_3 \rightarrow (NH4)_2SO_4 \quad \text{(R4)}$$

The production of nitrate aerosol (ammonium nitrate) results from the combination of NO_x and NH_3 emissions and their atmospheric reactions.

Reactions (R5–R7) show how NO_3^- aerosol formation is related to both NO_x and NH_3 emissions. Firstly, nitric acid is produced in the gas phase:

$$NO_2(g) + OH(g) + M \rightarrow HNO_3(g) + M \quad \text{(R5)}$$

ACPD
10, 30731–30776, 2010

and during the night by

$$NO_2(g) + NO_3(g) \rightarrow N_2O_5 \quad \text{(R6)}$$

The hydrolysis of N_2O_5 on wet aerosol surfaces is an important pathway to convert NO_x into HNO_3 (Dentener and Crutzen, 1993; Riemer et al., 2003):

$$N_2O_5(g) + H_2O \rightarrow 2HNO_3 \quad \text{(R7)}$$

If sufficient ammonia is available to neutralize all sulfate, the residual amount of ammonia can neutralize nitric acid to form the ammonium nitrate aerosol:

$$NH_3(g) + HNO_3(g) \leftrightarrow NH_4NO_3(aq,s) \quad \text{(R8)}$$

Note that React. (8) is reversible. The distribution of ammonium nitrate between the gas and the aerosol phase strongly depends on the temperature and relative humidity (Seinfeld and Pandis 1998, and references therein).

The IPCC estimated SO_2, NO_x, NH_3 and BC emissions in Table 3 for Europe are calculated for the same domain for which the EMEP and REAS emissions are given. We clearly see in the EMEP inventory a decrease in the SO_2 emissions for Europe from 21.65 Tg (2000) to 16.68 Tg (2010), which is a reduction of 23%. A similar reduction of 20% is calculated by IPCC AR5 3PD. The reduction given by EMEP between 1990 and 2010 is significant, −29.02 Tg (−64%). As mentioned before, EMEP does not include BC emissions. Therefore we analyze in Table 3 the BC emissions of the IPCC AR5 inventory. For Europe between 1990 and 2000, IPCC AR5 3PD shows a reduction (−0.114 Tg, −11%) in the BC emissions; however, between 2000 and 2010 a small increase (0.028 Tg, 3%) is indicated. NO_x emissions are ∼10% (1.45 Tg) lower in 2010 compared to 2000. This reduction largely results from policy and technology realized in road transport (e.g. catalytic converters). Between 2000 and 2010 NH_3 emissions in the EMEP inventory have declined (−2.5%) due to the recent NH_3 emission abatement measures to combat eutrophication problems in Northwestern Europe.

ACPD
10, 30731–30776, 2010

3.4.2 North-East America

In Fig. 5b and Table 2 the trend of MODIS Level 2 AOD for 8 stations is presented. For 7 stations the trends are negative and for 1 station (Big Meadows) the trend is slightly positive (1%). The MODIS Level 3 trends for all 8 stations are negative and in general somewhat larger than for Level 2. For North-East USA we have three AERONET stations for which substantial Daily Level 2 data is available within the domain of interest, i.e. Walker Branch (1340 days), Cartel (1131 days) and CCNY (1208 days), see Table S4. For these three stations the trend in the AOD is negative, which corresponds with MODIS Level 2. Analyzing the AOD trend of AERONET Daily Level 2 for North America in Table S4, we see that for the majority of the 18 stations the trends are negative (13 in total). Only for Bratts Lake (Canada, Saskatchewan), Railroad Valley (Nevada) and Rimrock (Idaho) the trends are positive.

The explanation of the general AOD reduction in North America is related to the Clean Air Act Amendments of 1990, which have led to a reduction of SO_2 and NO_x emissions. In Table 3 we see that the IPCC AR5 3PD inventory for the USA indicates a decrease of −4.71 Tg (−24%) in the SO_2 emissions between 2000 and 2010. This is similar and a continuation of the decrease between 1990 and 2000 (−4.44 Tg). NO_x emissions between 2000–2010 decrease by −22% (−3.35 Tg) for the IPCC AR5 3PD inventory. Anthropogenic BC emissions are similar to those in Europe, somewhat increasing over the USA between 2000 and 2010, 0.028 Tg (6%).

3.4.3 East Asia

In Fig. 5c, we focus on East Asia by analyzing the AOD trends for 8 stations (Table 2). For 7 stations the MODIS Level 2 trends are positive (Hefei, Nuist, Taihu, Backgarden_GZ, Anmyon, Bac Giang and Xianghe), and only for Beijing the trend is negative (−0.24 AOD). Interesting is the difference between Xianghe (+0.052 AOD) and Beijing (−0.240 AOD), as the distance between the two stations is only around 55 km. Analyzing the AOD profile (not shown) we find that the number of successful AOD retrievals

ACPD
10, 30731–30776, 2010

for Xianghe (1076) is almost a factor 2 higher than for Beijing (562). A possible explanation for this may be that the Xianghe station is located in a rural area. Because of the location, the MODIS dark-target aerosol retrieval algorithm (Remer et al., 2005) allows more successful retrievals with higher accuracy. The trend in AOD of Daily Level 2 AERONET data in Table S4 also shows a negative trend for Beijing (−0.076). For Xianghe the AERONET Daily Level 2 trend is positive (0.030 AOD), which corroborates the MODIS Level 2 trend (0.052 AOD). The small negative/positive recent trends in China may be related to the implementation of the 11th Five Year Plan (2006–2010) of State Environment Protection Administration (SEPA), which requires power plants to implement new air pollution reduction technologies after 2006. This implies that even though industrial and urban activities leading to air pollution continue to increase, decreasing emissions factors to some degree offset the emission trends.

Comparing the MODIS Level 2 trends with Level 3, we see that the trend is different for three stations (Hefei, Beijing and Anmyon). One of the reasons could be that the number of successful retrievals in the Level 3 data is not sufficient, but as we do not have access to the actual sampling time of MODIS Level 3 data, it remains unclear why differences in the trends are found for these three stations.

Analyzing the emission trends of SO_2, NO_x, NH_3 and BC over Asia helps explain the general upward trends over China and India. Half of China's SO_2 emissions are attributed to the burning of coal, mostly by power plants, which are to a large degree located in the eastern part of the country where the large cities are situated. Between 2001 and 2005, SO_2 emissions still increased by 27% (11th Five Year Plan, SEPA, March 2006). Lu et al. (2010) found an increase in SO_2 of 53% between 2000 and 2006, with 85% in the north and 28% in the south of the country. SO_2 emissions in China do not show a strong seasonal cycle (Zhang et al., 2009), because of the continual energy production for industry and domestic usage.

The provinces Hebei (which surrounds Beijing) with ∼70 million people, Henan (which borders Hebei to the south) with ∼100 million people and Anhui (eastern part of China) with ∼60 million people are the regions in China were most SO_2 is emitted

ACPD
10, 30731–30776, 2010

(Streets and Waldhoff, 2000). Most of the BC emissions in China (mainly in the rural areas) are caused by residential combustion of coal and biofuels for heating and cooking purposes (Streets et al., 2001; Bond et al., 2004; Lei et al., 2010).

The IPCC SO_2, NO_x, NH_3 and anthropogenic BC emissions in Table 3 for Asia are calculated for the same domain for which the REAS emissions are given. For Asia the REAS inventory indicates an increase in SO_2 emissions between 2000 and 2010 of 9.66 Tg (23%), which is somewhat lower than by IPCC AR5 3PD (12.49 Tg, 36%). Yet the increase between 1990 and 2010 is similar for REAS (18.67 Tg, 55%) and IPCC AR5 3PD (17.17 Tg, 58%). A recent study by Lu et al. (2010) estimated a strong increase in SO_2 emissions over China after 2000 of 53%, with an annual growth rate of 7.3%. The growth slowed after 2006, due to the implementation of new emission reduction technologies (i.e. desulfurization) in power plants. In Table 3 we see that 44% of the total global SO_2 emissions in 2010 originate from Asia (IPCC AR5 3PD). This percentage is even higher for anthropogenic BC (57%). IPCC AR 3PD shows an increase in the anthropogenic BC emissions of 0.891 Tg (33%) between 2000 and 2010, which is a factor 2.5 higher than indicated by REAS (0.358 Tg 13%). Interesting to see is the decrease between 1990 and 2000 by REAS (−0.137 Tg, −5%).

REAS estimates an increase in NO_x emissions between 2000–2010 of 37% (6.77 Tg), which is similar to the increase calculated by IPCC AR 3PD (6.26 Tg). Zhang et al. (2009) found an increase in NO_x emissions of 57% between 2000–2005 in China. The strong increase in SO_2 and NO_x emissions in East Asia are mainly caused by the strong increase of fossil fuel combustion to generate electricity and by road transport. REAS calculates an increase in NH_3 emissions of 13% (3.5 Tg), which is due to an increase in fertilizer application (Klimont, 2001). This differs from Europe where livestock is the dominant source of NH_3.

Analyzing the SO_2, NO_x, NH_3 and BC changes between 2000 and 2010 in the different emission inventories for the regions considered helps explain the AODs changes and trends derived from MODIS, MISR and AERONET observations. The reduction of SO_2 and NO_x emissions in Europe and North America corroborate the general AOD

ACPD
10, 30731–30776, 2010

trends observed by the different instruments. The same applies to the increase of the SO_2, NO_x, NH_3 and BC emissions over Asia and the corresponding upward AOD trends, including some compensating effects from industrial activities, emission factors and the mix of pollutant emissions.

4 Conclusions

Our analysis indicates generally negative AOD trends from Monthly Level 3 MODIS and MISR products for Europe and North America, whereas for Asia we derive a largely upward trend between 2000–2009, in qualitative agreement with the results of previous studies by Zhang and Reid (2010), Lu et al. (2010), Remer et al. (2008) and Chylek et al. (2007). Our study shows that the negative trends over parts of Europe and North-East America are significant. The AOD trends derived from the Level 3 MODIS and MISR products for the different regions are generally consistent with those derived from Monthly Level 2 data of AERONET. The difference between AERONET Daily and Monthly Level 2 AOD trends appears to be minor. It is nevertheless difficult to draw firm conclusions based on Level 3 data products, because the sampling is highly non-uniform. Therefore we also analyzed Level 2 MODIS data products for three selected regions, i.e. the Central Mediterranean, North-East America and East Asia, for which ample data coverage is available. We find that the AOD trend over the Central Mediterranean is negative for 2000–2009 and corresponds well with MODIS Level 3 data. Also for North-East America the trend is generally negative, which corresponds with that derived from MODIS Level 3 data. It seems likely that the downward trends in AODs over Europe and North America are related to the implementation of air pollution legislation, which has resulted in a decrease in the emissions of SO_2, NO_x and other criteria pollutants and resulting aerosol concentrations. In East Asia the trends for Level 2 data are positive at 8 stations, probably related to the increasing demand for energy and by growing industrial and urban activities (e.g. traffic), and associated increases in the emissions of SO_2, NO_x, BC and other pollutants. In East Asia the emission increases

ACPD
10, 30731–30776, 2010

and AOD trends after 2000 appear to have been moderated by a reduction of emission factors related to improved technology. The SSA trends over the USA appear to be negative for 8 locations, which indicate that relatively more light-absorbing aerosols are found. This suggests a stronger reduction of anthropogenic sulfur and nitrogen-containing aerosol precursor emissions relative to black carbon emissions, or even an increase of the latter, as also indicated by the emission estimates. This contrasts to the overall trend in Europe where the SSA might have increased since 2000 associated with decreasing black carbon emissions. The analysis of emission inventories indicates that AOD trends are generally dominated by changing anthropogenic SO_2 emissions, although probably more strongly in the 1990s than in the 2000s, in particular in Europe and Asia. Considering the importance of SO_2 emissions, the solar brightening in Europe by the negative AOD trends may have been stronger in the 1990s than in the 2000s. In Asia SO_2 emission increases appear to have decelerated recently, while those of NO_x have accelerated, which may lead to compensating tendencies in AOD, especially because NH_3 emissions have also increased (promoting the formation of ammonium nitrate).

Thus having derived consistent AOD trends from multiple data sources at many locations and linked these trends with emission histories, a next step would be to explore the connections between emissions and AODs more quantitatively with chemical transport models.

Supplementary material related to this article is available online at: http://www.atmos-chem-phys-discuss.net/10/30731/2010/acpd-10-30731-2010-supplement.pdf.

Acknowledgements. We are grateful for the helpful comments and suggestions by Ralph Kahn of NASA Goddard Space Flight Center. We thank the Principal Investigators of the AERONET network for the sun photometer data. The UK Natural Environment Research Council who have funded the instrument and the collection of the data of the Chilbolton station; the Laboratory of Atmospheric Physics, Aristotle University of Thessalonik; Dr. Serm Janjai, Department of

ACPD
10, 30731–30776, 2010

Physics, Silpakorn University, Thailand; the Research Center for Environmental Changes, Academic Sinica (RCEC) in Taiwan and the AEROCAN network which is the Canadian sub-network of AERONET. We also thank the MODIS Science Data Support Team and the Earth Observing System Data Gateway for processing and distributing the MODIS data. The MISR data were obtained from the NASA Langley Research Center Atmospheric Sciences Data Center. We acknowledge support by the European Research Council to the C8 project.

References

Abdou, W. A., Diner, D. J., Martonchik, J. V., Bruegge, C. J., Kahn, R. A., Gaitley, B. J., Crean, K. A., Remer, L. A., and Holben, B.: Comparison of coincident multiangle imaging spectroradiometer and moderate resolution imaging spectroradiometer aerosol optical depths over land and ocean scenes containing aerosol robotic network sites, J. Geophys. Res., 110, D10S07, doi:10.1029/2004JD004693, 2005.

Bond, T. C., Streets, D. G., Fernandes, S. D., Nelson, S. M., Yarber, K. F., Woo, J.-H., and Klimont, Z.: A technology-based global inventory of black and organic carbon emissions from combustion, J. Geophys. Res., 109, D14203, doi:10.1029/2003JD003697, 2004.

Bond, T. C., Bhardwaj, E., Dong, R., Jogani, R., Jung, S., Roden, C., Streets, D. G., Fernandes, S., and Trautmann, N.: Historical emissions of black and organic carbon aerosol from energy-related combustion, 1850–2000, with new emissions factors developed in collaboration with Liousse, C. Global Biogeochem. Cy., 21, GB2018, doi:10.1029/2006GB002840, 2007.

Buhaug, Ø., Corbett, J. J., Endresen, Ø., Eyring, V., Faber, J., Hanayama, S., Lee, D. S., Lee, D., Lindstad, H., Markowska, A. Z., Mjelde, A., Nelissen, D., Nilsen, J., Pålsson, C., Winebrake, J. J., and Wu, W.-Q., and Yoshida, K.: Second IMO GHG study 2009, International Maritime Organization (IMO) London, UK, 2009.

Chylek, P., Lohmann, U., Dubey, M., Mishchenko, M., Kahn, R., and Ohmura, A.: Limits on climate sensitivity derived from recent satellite and surface Observations, J. Geophys. Res., 112, D24S04, doi:10.1029/2007JD008740, 2007.

Cofala, J., Amann, M., Gyarfas, F., Schoepp, W., Boudri, J. C., Hordijk, L., Kroeze, C., Junfeng, L., Lin, D., Panwar, T. S., Gupta, S.: Cost-effective control of SO_2 emissions in Asia, Journal of Environmental Management 72, 149–161, 2004.

ACPD

10, 30731–30776, 2010

Cox, R. A. and Penkett, S. A.: Photo-oxidation of atmospheric SO_2, Nature, 229, 486–488, doi:10.1038/229486a0, 1971.
Dayan, U., Ziv, B., Shoop, T., and Enzel, Y.: Suspended dust over South-Eastern Mediterranean and its relation to atmospheric circulations, Int. J. Climatol., 28(7), 915–924, doi:10.1002/joc.1587, 2008.
De Meij, A. and Lelieveld, J.: Evaluating aerosol optical properties observed by ground-based and satellite remote sensing over the Mediterranean and the Middle East in 2006, Atmos. Res., accepted, 2010.
Dentener, F. J. and Crutzen, P. J.: Reaction of N_2O_5 on tropospheric aerosols: impact on the global distributions of NO_x, O_3, and OH, J. Geophys. Res., 98, 7149–7163, 1993.
Dey, S. and Di Girolamo, L.: A climatology of aerosol optical and microphysical properties over the Indian subcontinent from 9 years (2000–2008) of Multiangle Imaging Spectroradiometer (MISR) data, J. Geophys. Res., 115, D15204, doi:10.1029/2009JD013395, 2010.
Di Girolamo, L., Bond, T. C., Bramer, D., Diner, D. J., Fettinger, F., Kahn, R. A., Martonchik, J. V., Ramana, M. V., Ramanathan, V., and Rasch, P. J.: Analysis of multiangle imaging spectro radiometer (MISR) aerosol optical depths over greater India during winter 2001–2004, Geophys. Res. Lett., 31, L23115, doi:10.1029/2004GL021273, 2004.
Diner, D. J., Beckert, J. C., Reilly, T. H., Bruegge, C. J., Conel, J. E., Kahn, R. A., Martonchik, J. V., Ackerman, T. P., Davies, R., Gerstl, S. A. W., Gordon, H. R., Muller, J.-P., Myneni, R. B., Sellers, P. J., Pinty, B., and Verstraete, M. M.: Multiangle imaging spectroradiometer (MISR) instrument description and experiment overview, IEEE T. Geosci. Remote, 36(4), 1072–1087, 1998.
Diner, D.J., Bull, M., Matthews, J., McDonald, D., Moroney, C., Paradise, S., and Smyth, M.: Data Products Specifications, Incorporating the Science Data Processing Interface Control Document, JPL D-13963, Revision R, Jet Propul. Lab., California Institute of Technology, Pasadena, California, USA, 2009.
Dubovik, O., Smirnov, A., Holben, B. N., King, M. D., Kaufman, Y. J., Eck, T. F., and Slutsker, I.: Accuracy assessments of aerosol optical properties retrieved from aerosol robotic network (AERONET) Sun and sky radiance measurements, J. Geophys. Res., 105, 9791–9806, 2000.
Eck, T. F., Holben, B. N., Reid, J. S., Dubovik, O., Smirnov, A., O'Neill, N. T., Slutsker, I., and Kinne, S.: Wavelength dependence of the optical depth of biomass burning, urban and desert dust aerosols, J. Geophys. Res., 104, 31333–31350, 1999.

ACPD
10, 30731–30776, 2010

Eyring, V., Isaksen, I. S. A., Berntsen, T., Collins, W. J., Corbett, J. J., Endresen, O., Grainger, R. G., Moldanova, J., Schlager, H., and Stevenson, D. S.: Transport impacts on atmosphere and climate: Shipping, Atm. Env., 44, 4735–4771, doi:10.1016/j.atmosenv.2009.04.059, 2010.

Garg, A., Shukla, P. R., Bhattacharya, S., and Dadhwal, V. K.: Sub-region (district) and sector level SO_2 and NO_x emissions for India: assessment of inventories and mitigation flexibility, Atmos. Environ., 35, 703–713, 2001.

Gilgen, H., Wild, M., and Ohmura, A.: Means and trends of shortwave irradiance at the surface estimated from GEBA, J. Climate, 11, 2042–2061, 1998.

Heymsfield, A. J. and McFarquhar, G. M.: Microphysics of INDOEX clean and polluted trade cumulus clouds, J. Geophys. Res., 106(D22), 28653–28674, 2001.

Hinkelman, L. M., Stackhouse Jr., P. W., Wielicki, B. A., Zhang, T., and Wilson, S. R.: Surface insolation trends from satellite and ground measurements: comparisons and challenges, J. Geophys. Res., 114, D00D20, doi:10.1029/2008JD011004, 2009.

Intergovernmental Panel on Climate Change: Climate Change 2007, The Fourth IPCC Assessment Report, The Intergovernmental Panel on Climate Change, Cambridge Univ. Press, Cambridge, 2007.

Kahn, R. A., Gaitley, B., Martonchik, J., Diner, D., Crean, K., and Holben, B.: MISR global aerosol optical depth validation based on two years of coincident AERONET observations, J. Geophys. Res., 110, D10S04, doi:10.1029/2004JD004706, 2005.

Kahn, R. A., Nelson, D. L., Garay, M., Levy, R. C., Bull, M. A., Diner, D. J., Martonchik, J. V., Paradise, S. R., and Hansen, E. G., and Remer, L. A.: MISR aerosol product attributes, and statistical comparisons with MODIS, IEEE T. Geosci. Remote, 47(12), 4095–4114, 2009.

Kahn, R. A., Gaitley, B. J., Garay, M. J., Diner, D. J., Eck, T. F., Smirnov, A., and Holben, B. N.: MISR global aerosol product assessment by comparison with AERONET, J. Geophys. Res., 115, D23209, doi:10.1029/2010JD014601.

Kaufman, Y. J., Tanré, D., Remer, L. A., Vermote, E. F., Chu, A., and Holben, B. N.: Operational remote sensing of tropospheric aerosols over land form EOS-moderate resolution imaging spectroradiometer, J. Geophys. Res., 102, 17051–17065, 1997.

Kaufman, Y. J., Tanré, D., and Boucher, O.: A satellite view of aerosols in the climate system, Nature, 419, 215–223, 2002.

Kishcha, P., Starobinets, B., Kalashnikova, O., Long, C. N., and Alpert, P.: Variations of meridional aerosol distribution and solar dimming, J. Geophys. Res., 114, D00D14, doi:10.1029/2008JD010975, 2009.

ACPD
10, 30731–30776, 2010

Klimont, Z.: Current and future emissions of ammonia in China, in: Proceedings of the 10th International Emission Inventory Conference "One Atmosphere, One Inventory, Many Challenges", Denver, CO, 30 April–3 May 2001, available at: http://www.epa.gov/ttn/chief/conference/ei10/index.html, last accessed 15 December 2010, 2009.

Lamarque, J.-F., Bond, T. C., Eyring, V., Granier, C., Heil, A., Klimont, Z., Lee, D., Liousse, C., Mieville, A., Owen, B., Schultz, M. G., Shindell, D., Smith, S. J., Stehfest, E., Van Aardenne, J., Cooper, O. R., Kainuma, M., Mahowald, N., McConnell, J. R., Naik, V., Riahi, K., and van Vuuren, D. P.: Historical (1850–2000) gridded anthropogenic and biomass burning emissions of reactive gases and aerosols: methodology and application, Atmos. Chem. Phys., 10, 7017–7039, doi:10.5194/acp-10-7017-2010, 2010.

Lee, D. S., Pitari, G., Grewe, V., Gierens, K., Penner, J. E., Petzold, A., Prather, M. J., Schumann, U., Bais, A., Berntsen, T., Iachetti, D., Lim, L. L., and Sausen, R.: Aviation and global climate change in the 21st century, Atmos. Environ., 44, 4678–4734, doi:10.1016/j.atmosenv.2009.04.024, 2009.

Lei, Y., Zhang, Q., He, K. B., and Streets, D. G.: Primary aerosol emission trends for China, 1990–2005, Atmos. Chem. Phys. Discuss., 10, 17153–17212, doi:10.5194/acpd-10-17153-2010, 2010.

Lelieveld, J., Crutzen, P. J., Andreae, M. O., Brenninkmeijer, C. A. M., Campos, T., Cass, G. R., Dickerson, R. R., Fischer, H., de Gouw, J. A., Hansel, A., Jefferson, A., Kley, D., de Laat, A. T. J., Lal, S., Lawrence, M. G., Lobert, J. M., Mayol-Bracero, O., Mitra, A. P., Novakov, T., Oltmans, S. J., Prather, K. A., Ramanathan, V., Reiner, T., Rodhe, H., Scheeren, H. A., Sikka, D., and Williams, J.: The Indian Ocean experiment: widespread air pollution from South and South-East Asia, Science, 291, 1031–1036, 2001.

Leon, J.-F., Chazette, P., Dulac, F., Pelon, J., Flamant, C., Bonazzola, M., Foret, G., Alfaro, S. C., Cachier, H., Cautenet, S., Hamonou, E., Gaudichet, A., Gomes, L., Rajot, J.-L., Lavenu, F., Inamdar, S. R., Sarode, P. R., and Kadadevarmath, J. S.: Large-scale advection of continental aerosols during INDOEX, J. Geophys. Res., 106, 28427–28439, 2001.

Levy, R. C., Remer, L. A., Kleidman, R. G., Mattoo, S., Ichoku, C., Kahn, R., and Eck, T. F.: Global evaluation of the collection 5 MODIS dark-target aerosol products over land, Atmos. Chem. Phys., 10, 10399–10420, doi:10.5194/acp-10-10399-2010, 2010.

Long, C. N., Dutton, E. G., Augustine, J. A., Wiscombe, W., Wild, M., McFarlane, S. A., and Flynn, C. J.: Significant decadal brightening of downwelling shortwave in the continental United States, J. Geophys. Res., 114, D00D06, doi:10.1029/2008JD011263, 2009.

ACPD
10, 30731–30776, 2010

Lu, Z., Streets, D. G., Zhang, Q., Wang, S., Carmichael, G. R., Cheng, Y. F., Wei, C., Chin, M., Diehl, T., and Tan, Q.: Sulfur dioxide emissions in China and sulfur trends in East Asia since 2000, Atmos. Chem. Phys., 10, 6311–6331, doi:10.5194/acp-10-6311-2010, 2010.

Martonchik, J. V., Kahn, R. A., and Diner, D. J.: Retrieval of aerosol properties over land using MISR observations, in: Satellite Aerosol Remote Sensing Over Land, edited by: Kokhanovsky, A. A. and de Leeuw, G., Springer, Berlin, Germany, 267–293, 2009.

Mishchenko, M. I., Geogdzhayev, I. V., Rossow, W. B., Cairns, B., Carlson, B. E., Lacis, A. A., Liu, L., and Travis, L. D.: Long-term satellite record reveals likely recent aerosol trend, Science, 315, 1543, 2007.

Norris, J. R. and Wild, M.: Trends in aerosol radiative effects over China and Japan inferred from observed cloud cover, solar "dimming," and solar "brightening," J. Geophys. Res., 114, D00D15, doi:10.1029/2008JD011378, 2009.

Nurrohim, A. and Sakugawa, H.: A fuel-based inventory of NO_x and SO_2 emissions from manufacturing industries in Hiroshima Prefecture, Japan, Appl. Energ., 78(4), 355–369, doi:10.1016/j.apenergy.2003.10.003, 2004.

Ohara, T., Akimoto, H., Kurokawa, J., Horii, N., Yamaji, K., Yan, X., and Hayasaka, T.: An Asian emission inventory of anthropogenic emission sources for the period 1980–2020, Atmos. Chem. Phys., 7, 4419–4444, doi:10.5194/acp-7-4419-2007, 2007.

Ohmura, A.: Observed decadal variations in surface solar radiation and their causes, J. Geophys. Res., 114, D00D05, doi:10.1029/2008JD011290, 2009.

Pandis, S. N. and Seinfeld, J. H.: Sensitivity analysis of a chemical mechanism for aqueous-phase atmospheric chemistry, J. Geophys. Res., 94, 1105–1126, 1989.

Pinker, R. T., Zhang, B., and Dutton, E. G.: Do satellites detect trends in surface solar radiation?, Science, 308, 5723, 850–854, doi:10.1126/science.1103159, 2005.

Ramanathan, V., Crutzen, P. J., Lelieveld, J., Mitra, A. P., Althausen, D., Anderson, J., Andreae, M. O., Cantrell, W., Cass, G. R., Chung, C. E., Clarke, A. D., Coakley, J. A., Collins, W. D., Conant, W. C., Dulac, F., Heintzenberg, J., Heymsfield, A. J., Holben, B., Howell, S., Hudson, J., Jayaraman, A., Kiehl, J. T., Krishnamurti, T. N., Lubin, D., McFarquhar, G., Novakov, T., Ogren, J. A., Podgorny, I. A., Prather, K., Priestley, K., Prospero, J. M., Quinn, P. K., Rajeev, K., Rasch, P., Rupert, S., Sadourny, R., Satheesh, S. K., Shaw, G. E., Sheridan, P., and Valero, F. P. J.: The Indian Ocean experiment: an integrated analysis of the climate forcing and effects of the great Indo-Asian haze, J. Geophys. Res., 106, 28371–28398, 2001a.

Ramanathan, V.. Crutzen, P. J., Kiehl, J. T., and Rosenfeld, D.: Aerosols, climate, and the

ACPD
10, 30731–30776, 2010

hydrological cycle, Science 294, 2119–2124, 2001b.
Remer, L. A., Kleidman, R. G., Levy, R. C., Kaufman, Y. J., Tanre, D., Mattoo, S., Martins, J. V., Ichoku, C., Koren, I., Yu, H., and Holben, B. N.: Global aerosol climatology from the MODIS satellite sensors, J. Geophys. Res., 113, doi:10.1029/2007JD009661, 2008.
Remer, L. A., Kaufman, Y. J., Tanré, D., Mattoo, S., Chu, D. A., Martins, J. V., Li, R.-R., Ichou, C., Levy, R. C., Kleidman, R. G., Eck, T. F., Vermote, E., and Holben, B. N.: The MODIS Aerosol Algorithm, Products, and Validation, J. Atmos, Sci., Special Section, 62, 947–973, 2005.
Riemer, N., Vogel, H., Schell, B., Ackermann, I., Kessler, C., and Hass, H.: Impact of the heterogeneous hydrolysis of N_2O_5 on chemistry and nitrate aerosol formation in the lower troposphere under photosmog conditions, J. Geophys. Res., 108(D4), 4144, doi:10.1029/2002JD002436, 2003.
Seinfeld, J. H. and Pandis, S. N.: Atmospheric Chemistry and Physics, Wiley, New York, 1998.
SEPA (State Environment Protection Administration of China): 11th Five Year Plan, 2006–2010, Rev. Environ. Econ. Policy (2009), 3(2), 231–250, doi:10.1093/reep/rep006, released March 2006.
Smith et al.: updated from Smith, S. J., Pitcher, H., and Wigley, T. M. L.: Global and regional anthropogenic sulfur dioxide emissions, Global Planet. Change, 29(1–2), 99–119, 2001; Smith, S. J., Andres, R., Conception, E., and Lurz, J.: Sulfur Dioxide Emissions: 1850–2000, JGCRI Report, 2004; PNNL-14537, 2010.
Streets, D. G. and Waldhoff, S. T.: Present and future emissions of air pollutants in China: SO_2, NO_x, and CO, Atmos. Environ., 34(3), 363–374, 2000.
Streets, D. G., Gupta, S., Waldhoff, S. T., Wang, M. Q., Bond, T. C., and Yiyun, B.: Black carbon emissions in China, Atmos. Environ., 35(25), 4281–4296, 2001.
Streets, D. G., Wu, Y., and Chin, M.: Two-decadal aerosol trends as a likely explanation of the global dimming/brightening transition, Geophys. Res. Lett., 33, L15806, 2006.
Streets, D. G., Yan, F., Chin, M., Diehl, T., Mahowald, N., Schultz, M., Wild, M., Wu, Y., and Yu, C.: Anthropogenic and natural contributions to regional trends in aerosol optical depth, 1980–2006, J. Geophys. Res., 114, D00D18, doi:10.1029/2008JD011624, 2009.
Tanré, D., Kaufman, Y. J., Herman, M., and Mattoo, S.: Remote sensing of aerosol properties over oceans using the MODIS/EOS spectral radiances, J. Geophys. Res., 102, 16971–16988, 1997.
Vestreng, V., Myhre, G., Fagerli, H., Reis, S., and Tarrasón, L.: Twenty-five years of contin-

ACPD
10, 30731–30776, 2010

uous sulphur dioxide emission reduction in Europe, Atmos. Chem. Phys., 7, 3663–3681, doi:10.5194/acp-7-3663-2007, 2007.
Vestreng, V., Ntziachristos, L., Semb, A., Reis, S., Isaksen, I. S. A., and Tarrasón, L.: Evolution of NO_x emissions in Europe with focus on road transport control measures, Atmos. Chem. Phys., 9, 1503–1520, doi:10.5194/acp-9-1503-2009, 2009.
Van Vuuren, D., den Elzen, M., Lucas, P., Eickhout, B., Strengers, B., van Ruijven, B., Wonink, S., and van Houdt, R.: Stabilizing greenhouse gas concentrations at low levels: an assessment of reduction strategies and costs, Climatic Change, 81, 119–159, doi:10.1007/s/10584-006-9172-9, 2007.
Weatherhead, E. C., Reinsel, G. C., Tiao, G. C., Meng, X., Choi, D., Cheang, W., Keller, T., DeLuisi, J., Wuebbles, D. J., Kerr, J. B., Miller, A. J., Oltmans, S. J., and Frederick, J. E.: Factors affecting the detection of trends: statistical considerations and applications to environmental data, J. Geophys. Res., 103, 17149–17161, 1998.
Wild, M.: Introduction to special section on Global Dimming and Brightening, J. Geophys. Res., 115, D00D00, doi:10.1029/2009JD012841, 2010.
Zhang, J. and Reid, J. S.: A decadal regional and global trend analysis of the aerosol optical depth using a data-assimilation grade over-water MODIS and Level 2 MISR aerosol products, Atmos. Chem. Phys., 10, 10949–10963, doi:10.5194/acp-10-10949-2010, 2010.
Zhang, Q., Streets, D. G., Carmichael, G. R., He, K. B., Huo, H., Kannari, A., Klimont, Z., Park, I. S., Reddy, S., Fu, J. S., Chen, D., Duan, L., Lei, Y., Wang, L. T., and Yao, Z. L.: Asian emissions in 2006 for the NASA INTEX-B mission, Atmos. Chem. Phys., 9, 5131–5153, doi:10.5194/acp-9-5131-2009, 2009.

ACPD
10, 30731–30776, 2010

Table 1a. AOD trend by MODIS and MISR Level 3 monthly mean values for the period 2000–2009, based on 152 stations.

	MODIS trend (%)	MODIS trend absolute	MISR trend (%)	MISR trend absolute	Number of locations
Europe	−32	−0.060	−7	−0.010	39
Eastern Europe	−22	−0.050	−7	0.012	7
North America	−25	−0.043	−13	−0.017	40
South America	−11	−0.020	5	0.008	15
Africa	−18	−0.063	−6	−0.023	9
Asia	−2	−0.007	11	0.032	33
Australia	−43	−0.045	2	0.002	8
Middle East	31	0.098	19	0.065	3

ACPD
10, 30731–30776, 2010

Table 1b. AOD trend by MODIS (Level 3), MISR (Level 3) and AERONET (Level 2) for the period 2000–2009, based on 62 stations.

	MODIS trend (%)	MODIS trend absolute	MISR trend (%)	MISR trend absolute	AERONET (%)	AERONET absolute	Number of locations
Europe	−30	−0.060	−9	−0.014	−25	−0.054	17
Eastern Europe	−23	−0.047	−5	−0.008	−25	0.056	4
North America	−23	−0.039	−10	−0.014	−24	−0.033	19
South America	−9	−0.0185	−6	−0.0011	−14	−0.030	7
Africa	−23	−0.110	−7	−0.033	4	0.020	4
Asia	−1	−0.0065	15	0.050	52	0.165	7
Australia	−40	−0.054	−2	−0.0022	−62	−0.092	2
Middle East	23	0.072	5	0.0145	33	0.063	2

ACPD
10, 30731–30776, 2010

Table 2. Change in AOD between 2000–2009 using MODIS Level 2 data for the Central Mediterranean, North-East USA and Eastern Asia.

Station	Change in AOD MODIS L2	Number valid observations	Change in AOD MODIS L3	Number valid observations
Central Mediterranean				
Ispra	−0.084 ; −31%	858	−0.086 ; −28%	118
Forth Crete	−0.080 ; −28%	682	−0.047 ; −20%	119
Rome Tor Vergata	−0.075 ; −26%	1052	−0.060 ; −28%	119
Venice	−0.048 ; −18%	596	−0.107 ; −33%	118
Thessaloniki	−0.169* ; −43%	749	−0.085 ; −31%	119
Lecce University	−0.054 ; −26%	373	−0.027 ; −13%	118
IMS−METU−ERDEMLI	−0.072 ; −25%	571	−0.038 ; −14%	118
North−East America				
Havard Forest	−0.011 ; −7%	467	−0.050 ; −39%	119
Burtonsville	−0.079 ; −30%	863	−0.085 ; −37%	119
Calipso Wilston LK	−0.087 ; −31%	703	−0.082 ; −34%	119
Big Meadows	0.002 ; 1%	673	−0.094 ; −50%	119
Columbia Science Centre	−0.030 ; −16%	828	−0.082 ; −43%	119
Walker Branch	−0.023 ; −11%	854	−0.062 ; −34%	119
CCNY	−0.126 ; −25%	244	−0.042 ; −19%	118
Cartel	−0.025 ; −14%	330	−0.031 ; −26%	118
North−East Asia				
Hefei	0.0023 ; 1%	741	−0.025 ; −3%	118
Nuist	0.218 ; 26%	484	0.018 ; 3%	119
Taihu	0.647 ; 100%	124	0.171 ; 23%	118
Beijing	−0.24 ; −24%	562	0.060 ; 11%	118
BackgardenGZ	0.117 ; 14%	615	0.124 ; 23%	119
Anmyon	0.052 ; 10%	273	−0.019 ; −5%	118
Bac Giang	0.191 ; 27%	497	0.087 ; 19%	118
Xianghe	0.052 ; 1%	1076	0.06 ; 11%	118

* Two outliers in the AOD for Thessaloniki are observed, on 4 Apr 2000 (1.611) and on 24 Aug 2000 (1.967). Excluding these values result in the change of −0.12 (−33%).

ACPD
10, 30731–30776, 2010

Table 3. Total emissions of SO_2 (a), anthropogenic BC (b), NH_3 (c) and NO_x (d) in Tg yr^{-1} for 1990, 1995, 2000, 2005 and 2010 for Europe, Asia, North America (USA) and globally.

Dataset	1990	1995	2000	2005	2010
(a) SO_2 Tg yr^{-1}					
Europe					
EMEP	45.7	29.31	21.65	18.51	16.68
IPCC RCP 3PD	44.13		22.51	21.34	18.07
Asia					
REAS	33.71	41.17	42.72	52.65	52.38
IPCC RCP 3PD	29.77		34.45	40.54	46.94
USA					
IPCC RCP 3PD	23.77		19.33	17.41	14.62
Global					
IPCC RCP 3PD	127.4		106.9	109.5	107.2
(b) BC Tg yr^{-1}					
Europe					
IPCC RCP 3PD	0.995		0.879	0.915	0.907
Asia					
REAS	2.860	2.958	2.723	2.902	3.081
IPCC RCP 3PD	2.480		2.699	y3.180	3.590
USA					
IPCC RCP 3PD	0.466		0.4532	y0.4660	0.4812
Global					
IPCC RCP 3PD	4.909		5.150	y5.767	6.220
(c) NH_3 Tg yr^{-1}					
Europe					
EMEP	8.997	7.324	7.110	7.085	6.936
IPCC RCP 3PD	7.938		8.292	8.117	8.066
Asia					
REAS	22.96	26.27	28.10	29.31	31.60
IPCC RCP 3PD	18.48		16.73	18.00	19.42
USA					
IPCC RCP 3PD	4.305		4.411	4.545	4.682
Global					
IPCC RCP 3PD	42.61		37.46	39.39	41.69
(d) NO_x (NO Tg yr^{-1})					
Europe					
EMEP	18.65	15.61	14.22	14.13	12.77
IPCC RCP 3PD	18.64		15.63	15.76	14.21
Asia					
REAS	11.68	15.67	18.18	22.34	24.95
IPCC RCP 3PD	15.28		18.70	21.80	24.96
USA					
IPCC RCP 3PD	15.71		15.35	13.29	12.00
Global					
IPCC RCP 3PD	67.65		68.41	69.69	70.25

ACPD
10, 30731–30776, 2010

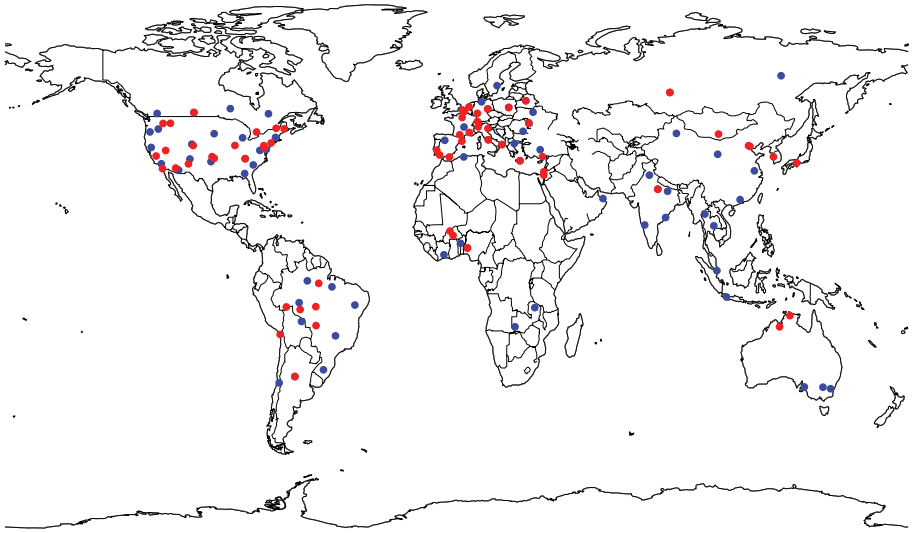

Fig. 1. Overview of the AERONET stations for which monthly mean AODs are compared with MODIS and MISR AOD (red dots). The blue dots represent locations for which only the AOD trends between MODIS and MISR are compared. All comparisons are for the period 2000–2009.

ACPD
10, 30731–30776, 2010

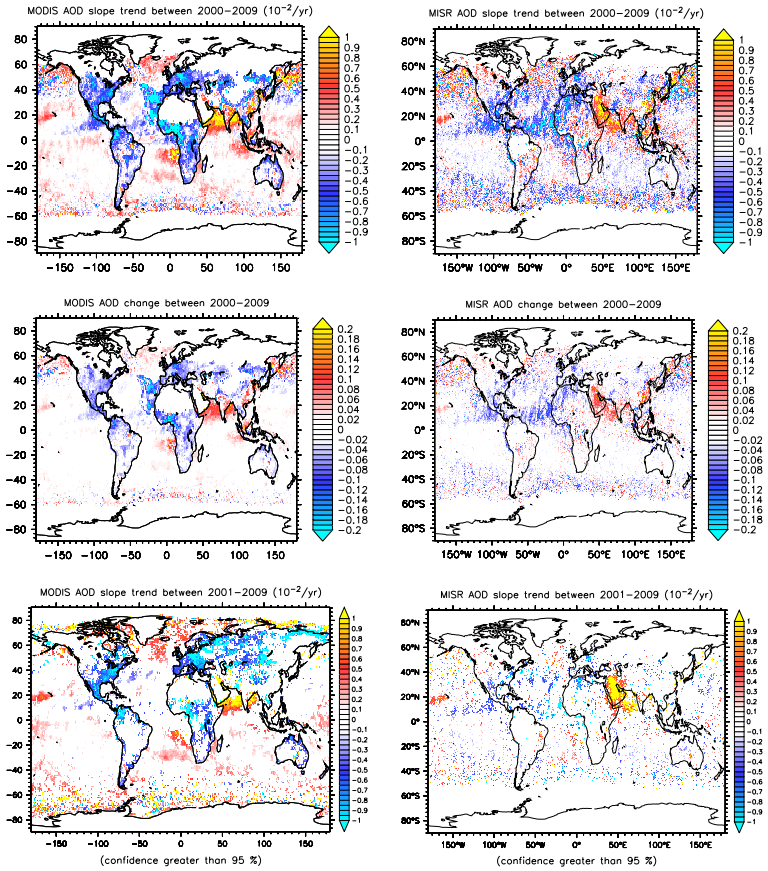

Fig. 2. MODIS **(a)** and MISR **(b)** linear AOD trend between 2000 and 2009, **(c)** and **(d)** the difference in AOD based on the linear trends by MODIS and MISR, respectively, followed by MODIS **(e)** and MISR **(f)** Level 3 AOD trend between 2001 and 2009 with confidence level >95% **(c)**. This analysis is based on monthly mean MODIS and MISR Level 3 products.

ACPD
10, 30731–30776, 2010

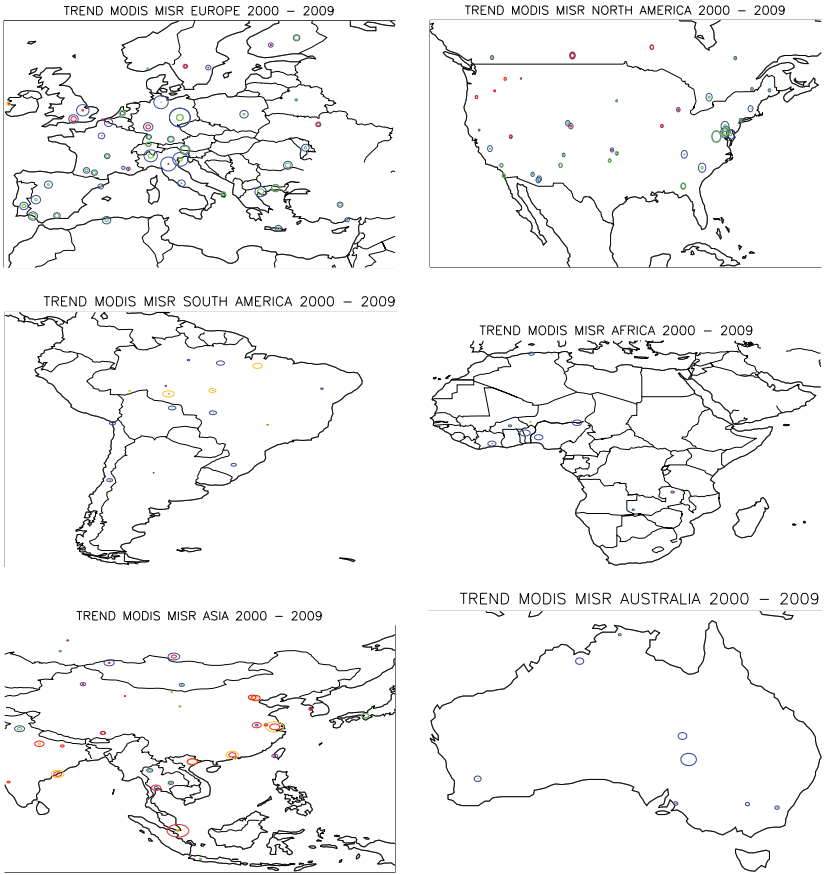

Fig. 3. AOD trends by MODIS and MISR, based on Level 3 data products, for Europe **(a)**, North America **(b)**, South America **(c)**, Africa **(d)**, Asia **(e)** and Australia **(f)**. Blue circles represent MODIS negative trends, green circles MISR negative trends, orange MODIS positive trends and red MISR positive trends. The size of the circles indicates the magnitude of the trends.

ACPD
10, 30731–30776, 2010

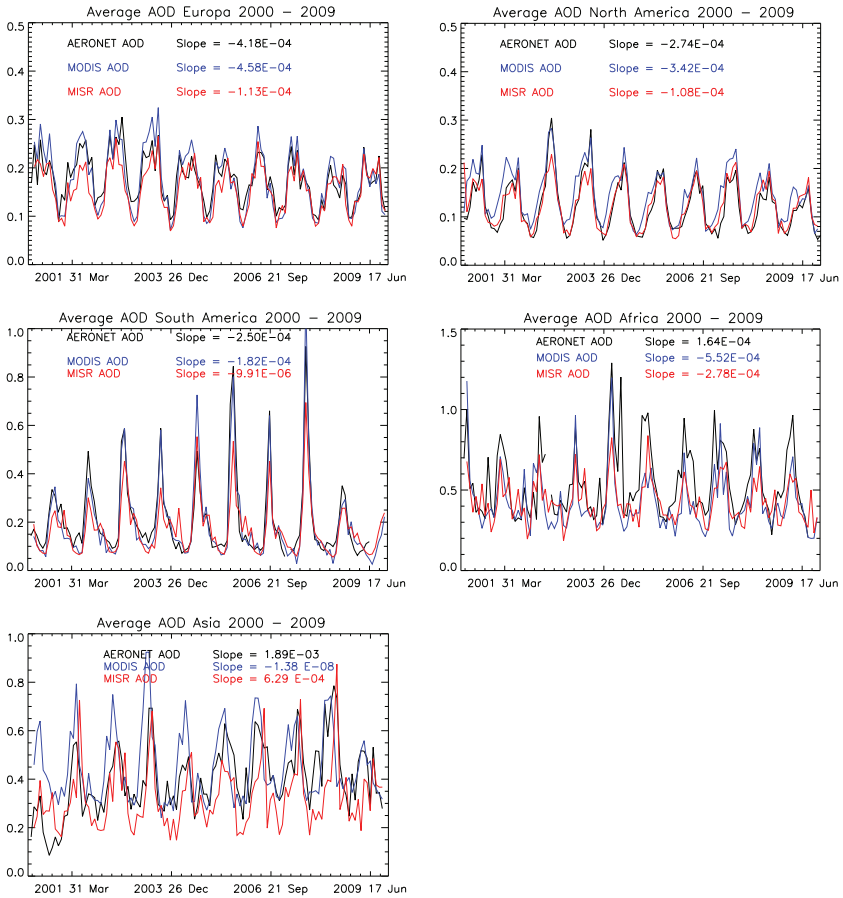

Fig. 4. Average AOD temporal profiles by MODIS (Level 3), MISR (Level 3) and AERONET (Level 2) for the period 2000–2009 for Europe, North America, South America, Asia, Africa and Australia, together with the slopes of the linear trends.

ACPD
10, 30731–30776, 2010

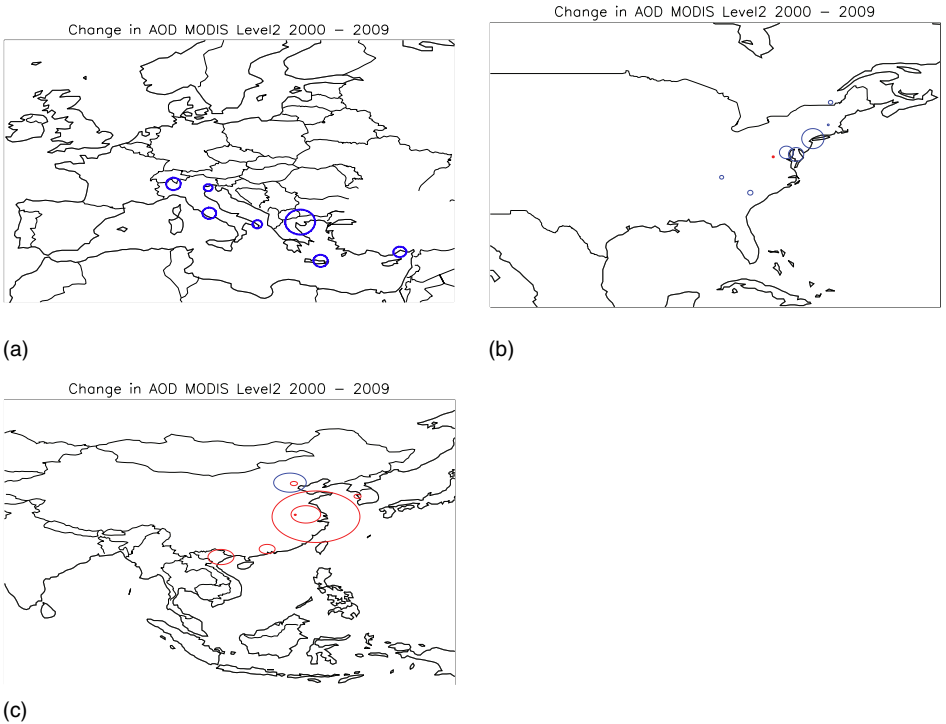

Fig. 5. Change in AOD for MODIS Level 2 data between 2000 and 2009 for Central Mediterranean **(a)**, North-East USA **(b)** and North-East China **(c)**. Red indicates positive and blue negative changes.

ACPD
10, 30731–30776, 2010